

A Topological Classification of Finite Chiral Structures using Complete Matchings

Maxine M. McCarthy and D. M. Whittaker
University of Sheffield
(Dated: May 28, 2024)

We present the theory and experimental demonstration of a topological classification of finite tight binding Hamiltonians with chiral symmetry. Using the graph-theoretic notion of complete matchings, we show that many chiral tight binding structures can be divided into a number of sections, each of which has independent topological phases. Hence the overall classification is $N\mathbb{Z}_2$, corresponding to 2^N distinct phases, where N is the number of sections with a non-trivial \mathbb{Z}_2 classification. In our classification, distinct topological phases are separated by exact closures in the energy spectrum of the Hamiltonian, with degenerate pairs of zero energy states. We show that these zero energy states have an unusual localisation across distinct regions of the structure, determined by the manner in which the sections are connected together. We use this localisation to provide an experimental demonstration of the validity of the classification, through radio frequency measurements on a coaxial cable network which maps onto a tight binding system. The structure we investigate is a cable analogue of an ideal graphene ribbon, which divides into four sections and has a $4\mathbb{Z}_2$ topological classification.

I. INTRODUCTION

Topology has become ubiquitous in modern physics, with many lattice structures and materials shown to have non-trivial topological attributes. A topological material is characterised by properties which remain unchanged during adiabatic evolution, making them robust in the presence of disorder. For instance, boundary states in one-dimensional topological lattices may have energies which are resistant to disorder [1], while in two-dimensions they may provide directional transport which is protected against backscattering [2–5]. In order to investigate these potentially useful properties, it is necessary to be able to classify the different topological phases of a given Hamiltonian.

Distinct topological phases are generally understood from two perspectives. The first is that two phases are distinct if, and only if, they cannot be related by (symmetry respecting) adiabatic evolution. The second is that a non-trivial topological phase has interesting boundary properties. The first perspective allows us to assign topological indices to distinct phases, and the second gives a physical significance to a classification. Both are connected by the famous bulk-boundary correspondence [6] which, since the discovery that the quantum Hall effect is topological [2, 7] has proven a powerful tool for the prediction of topological boundary phenomena. Most approaches to classification make use of the bulk-boundary correspondence in some way.

A ubiquitous topological classification is that of the 10-fold way [8], in which K-theoretic methods are used to classify each of the Altland-Zirnbauer (AZ) symmetry classes of momentum-space Hamiltonians [9]. Another approach is topological quantum chemistry [10, 11], where the classification is obtained by looking for topologically non-trivial states. In particular, the presence of states which cannot be adiabatically deformed to the atomic limit indicates a topologically non-trivial band in the bulk [12]. These methods provide a classification of

stable and fragile topological phases in a huge number of systems [13].

A useful approach for strong disorder relies on defining a non-commutative Brillouin zone [14–16]. Using non-commutative geometry, the Brillouin zone is modified to allow for variations in each unit cell of the structure, by defining a configuration space for the set of distinct unit cells. Translational invariance is no longer required, giving a disordered bulk-boundary correspondence.

For finite structures, a spectral localiser [17, 18] can predict the presence of approximately zero energy boundary states (also by demonstrating states cannot be localised to an atomic limit), therefore classifying a structure via the converse of the bulk-boundary correspondence. Alternatively local realspace markers may be used [19, 20] whose average gives a topological index for the entire structure. While this averages to a quantised value in the thermodynamic limit, such local markers are not exactly quantised in finite structures.

It has been shown that finite size effects may cause a rich sequence of topological phase transitions, corresponding to gap closures separating *topological bubbles* [21] in inversion symmetric structures. The number of approximately zero energy boundary states in such a bubble takes an integer value corresponding to a \mathbb{Z} classification in finite, inversion-symmetric Hamiltonians. These states are resistant to small amounts of disorder. Such an approach has also been extended to time-reversal symmetric systems [22]. Alternatively the finite structure may be repeated as a periodic supercell [23, 24] allowing the use of momentum-space methods to classify the topological phases.

These approaches leave open a problem: how may a structure be classified when we completely lose the bulk-boundary correspondence? That is, we no longer have any way to define a boundary or a bulk. This situation may occur in a small finite structure, particularly with strong disorder and/or no underlying lattice structure (for instance, a random finite network). Strongly disor-

dered finite systems may have a non-trivial topological classification [17, 25, 26] although the number of distinct topological phases is not always clear, motivating a general approach to topologically classify finite structures which have lost the bulk-boundary correspondence. In this paper, we propose a partial solution to this problem. Using graph-theoretic methods, we give a topological classification for finite chiral symmetric structures. We achieve this by considering equivalence classes of finite real space Hamiltonians with arbitrary values for the hopping terms.

In a finite structure at sufficient disorder, a bulk may not be possible to define, however non-adiabatic evolution may still be defined. For a finite system, a closing in the energy spectrum is analogous to a band gap closing in momentum space. In structures with chiral symmetry, and thus a symmetric energy spectrum, this corresponds to the appearance of pairs of zero energy states. Determining the conditions on the hopping terms which lead to the presence of these states allows us to define equivalence classes of Hamiltonians. A similar approach to defining topological phase boundaries has been used in [17, 25, 26].

Using this definition of equivalence classes we find that many structures have a rich classification resulting from the fact that they can be divided into a number of *sections*, each of which can be assigned an independent topological phase. These sections are identified as corresponding to factors of the determinant. Such factors may be determined by the hopping terms that appear in the expansion of the determinant of the Hamiltonian, and therefore play a role in defining the conditions for zero energy states. Any other hopping terms in the Hamiltonian can be removed without affecting the classification. This removal process results in the structure separating into disconnected pieces, each constituting a section. For each section we can determine an independent 0 or \mathbb{Z}_2 classification, using a sub-Hamiltonian defined on the section.

The existence of sections depends on the connectivity of the network representing the hopping terms in the Hamiltonian. They can occur in structures with some regularity, as in the graphene related examples which are considered in this work. However, they can also appear in more randomly connected structures. Checking 154131 non-isomorphic graphs which represent some of the connected chiral structures with 18 sites or fewer, and using randomised searches on larger finite chiral structures, we find that the classification of a structure is the most rich when each site has an average of three hopping terms. For an average of two the underlying connectivity is generally too sparse to provide a rich classification, and at four or greater, the structure is often too constrained by its connectivity to allow the division into many sections.

Of the 154131 graphs classified, for all positive and real hopping terms, 14% had no distinct topological phases, with the remaining being topologically non-trivial. 82% had two topological phases, and 4% had 4 to 16 distinct topological phases, with only 18 of the classified graphs

having 16 phases. Including trivial and non-trivial sections 8% of structures has no sections, 68% had one section, and 24% had 2 to 9 sections (trivial sections can still affect physical properties, such as localisation).

The infinite and finite classification of the sub-Hamiltonian corresponding to a section may be different. Considering a section as a one-dimensional supercell of an infinite lattice a transfer matrix treatment leads to one trivial and one non-trivial topological phase, separated by a gap closure somewhere in the Brillouin zone. Hence, with this definition, every section has a \mathbb{Z}_2 classification. Furthermore, the classes AIII and BDI have a \mathbb{Z} classification using the 10-fold way. In this infinite interpretation, a section having a non-trivial topological phase results in boundary localised topologically robust zero modes to one end of that section. This gives a connection to higher order topology arising through stacked chiral structures.

We seek to classify the actual finite structure, so we adopt the convention that only unavoidable gap closures which are observable (corresponding to closure at zero momentum) separate topological phases. This means that some sections will have a \mathbb{Z}_2 classification, while others will be topologically trivial. The complete structure behaves as a stack of sections, connected together in such a way that the topological phase of each section is independent. This gives a classification as the direct sum $\bigoplus_1^N \mathbb{Z}_2 \cong N\mathbb{Z}_2$ where N is the number of sections with a non-trivial classification, and depends on the underlying connectivity of the structure. For periodic materials, the stacking is not unlike that seen in [27]. Others have also shown that a rich classification can follow from the underlying connectivity of a structure [28, 29].

We also show that the localisation of the zero energy states that accompany a topological phase transition is determined by the connections between the sections. We define a partial ordering of the sections based on this connectivity, such that each of the zero energy states created by making one section topologically marginal spreads in only one direction through the remaining sections. This provides an experimentally accessible verification of the existence of the sections. We perform such an experiment using a coaxial cable network, which has been shown to map onto a tight-binding Hamiltonian [26, 30–32]. The structure we consider is a zigzag ‘graphene’ nanoribbon consisting of four rows of sites, each of which forms a separate section, leading to a $4\mathbb{Z}_2$ classification.

We begin by discussing the theory behind the classification in section II before discussing experimental results in a small graphene structure in section III, and concluding in IV. Supplementary material is provided with more mathematical and experimental details.

II. CLASSIFYING FINITE CHIRAL STRUCTURES

Chiral symmetry is one of the fundamental symmetries of the Altland-Zirnbauer symmetry classes [9]. A chiral Hamiltonian H anticommutes with a unitary C , ensuring non-zero eigenvalues come in $\pm\varepsilon$ pairs. When allowing algebraically independent hopping terms (thereby letting the structure have arbitrary hopping disorder) a Hamiltonian with chiral symmetry necessarily has two sublattices of sites, which we label ‘black’ and ‘white’ (a consequence of the Hara-Sachs theorem [33, 34]). Each black site is only connected (through non-zero hopping terms) to white sites, and each white site is only connected to black sites. An example is shown in Fig. 1.

For a structure with n_B black sites and n_W white sites, there are always at least $|n_B - n_W|$ zero energy states. Since these exist independently of the values of the hopping terms in H , they are described as topologically protected states. Such states can also occur in structures with $n_B = n_W$. If a structure has such protected states, the determinant of the Hamiltonian is necessarily zero for all values of the hopping terms, so a classification based on the conditions for $|H| = 0$ is not possible. In this work, we consider only structures with equal numbers of black and sites and no topologically protected states.

Two Hamiltonians H_1 and H_2 , are considered to have a different topological phase if they cannot be related under adiabatic evolution. That is, there exists no continuous way to evolve between H_1 and H_2 without a gap closing in the spectrum. For a chiral Hamiltonian with an even number of sites, zero energy states necessarily occur in degenerate pairs. This degeneracy corresponds to a closed gap in the spectrum, indicating non-adiabatic evolution. Therefore finding the conditions for a singular Hamiltonian determines the topological phase boundaries in a finite structure.

To explore distinct topological phases on a finite chiral structure we consider a set of sites connected by non-zero hopping terms. Formally this defines a graph G . On G we

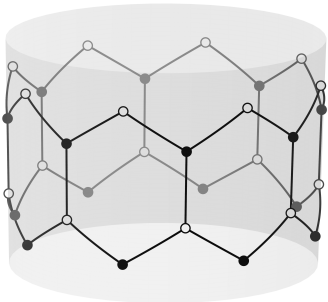


FIG. 1. A two row ribbon zigzag graphene, looped to form a cylinder. The structure has chiral symmetry, with the two sublattices indicated by the black and white sites. The topological classification of structures like this can be found using the methods we describe: this one is $2\mathbb{Z}_2$.

define a tight binding (TB) Hamiltonian, H , where each hopping term may be continuously evolved, algebraically independently. To ensure changes to G only include continuous evolution we do not allow new connections to be introduced, or existing connections to be broken. In terms of H , this means non-zero hopping terms must remain non-zero, and hopping terms which are zero cannot be modified. Otherwise we allow complete freedom to continuously evolve hopping terms of H , giving access to strongly disordered Hamiltonians defined on G . We do, however, restrict the hopping terms to be real: any topological phase boundary in a finite structure can be avoided, by evolving the Hamiltonian through a path involving complex hopping terms. Although we can allow negative values, the requirement for non zero real hopping terms means that they cannot change sign as they evolve.

The tuple of algebraically independent hopping terms on G , defines an affine space, ξ . Each Hamiltonian H on G defines a point in ξ . Continuously evolving hopping terms in H corresponds to following a path in ξ . We refer to ξ as the *parameter space* of G . Topological phase boundaries in ξ correspond to boundary free surfaces one dimension lower than ξ . An example of a slice of a parameter space is given in Fig. 3.

The classification problem can be completely reduced to finding solutions to $|H| = 0$, which necessarily corresponds to degenerate zero energy states. Although degeneracies can occur at non-zero energies, in a system with algebraically independent hopping terms, such a gap closure requires at least two constraints on the hopping terms, a consequence of the Hara-Sachs theorem [33, 34]. Such constraints are described by surfaces which are at least two dimensions lower than ξ , and therefore cannot divide it: they are always avoidable gap closures. This ensures topological phase boundaries are only given by a collection of surfaces in ξ corresponding to $|H| = 0$.

The Hamiltonian for a chiral structure has an anti-diagonal block basis corresponding to ordering the sites by sublattice,

$$H = \begin{pmatrix} 0 & Q \\ Q^\dagger & 0 \end{pmatrix}, \quad (1)$$

so the determinant $|H| = -|Q||Q^\dagger|$. For equal numbers of black and white sites, Q is a square matrix, so $|Q| = |Q^\dagger|$, and we can use either to determine the classification.

Every term in the expansion of Q is algebraically independent, so $|Q|$ is a multi linear form of the hopping terms. That is $|Q|$ varies linearly with respect to each hopping term in its expansion. For each hopping term in $|Q|$, solutions to $|Q| = 0$ follow from solving a linear equation, constraining exactly one hopping term. This ensures that every solution to $|Q| = 0$ corresponds to a surface in ξ which is both unbounded, and one dimension lower than that of the parameter space, splitting ξ in to distinct regions. This linear behaviour also ensures that $|Q|$ changes sign as we go over a phase boundary, meaning $\text{Sign}[|Q|]$ is a topological invariant [17]. This is in

contrast to $\text{Sign} [|H|]$, which does not change at a phase boundary.

To classify a structure, we must understand how to set $|Q|$ to zero by continuously evolving hopping terms, which may be done by finding the irreducible factors of $|Q|$. If a factorisation of $|Q| = \prod |q_i|$ exists, and it is possible to solve $|q_i| = 0$, then the factor $|q_i|$ defines a pair of distinct phases, where $\text{Sign} [|q_i|]$ is a topological invariant. We say such a factor is *non-trivial*. The classification of the structure is then given by $\bigoplus^N \mathbb{Z}_2 \cong N\mathbb{Z}_2$ where N is the number of non-trivial factors.

The determinant $|Q|$ defines a polynomial in a unique factorisation domain (details are given in the supplementary material section A) ensuring the maximum number of non-trivial factors, N , of $|Q|$ is also a topological invariant, so the classification is well defined. It is only possible to change N by removing or introducing new hopping terms or sites, that is, under discontinuous evolution of H .

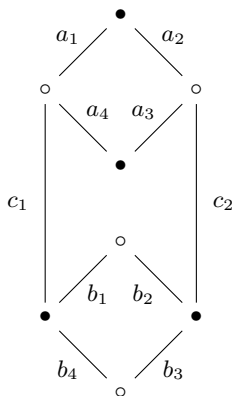


FIG. 2. A simple two row graphene zigzag structure with the hopping terms labelled as in Eq.(2). This structure has two sections and four distinct topological phases, corresponding to a $2\mathbb{Z}_2$ classification.

To show a simple example, we consider a 2 row zigzag graphene structure, with 4 sites on each row, see Fig. 2. This is described by the matrix

$$Q = \begin{pmatrix} a_1 & a_4 & c_1 & 0 \\ a_2 & a_3 & 0 & c_2 \\ 0 & 0 & b_1 & b_2 \\ 0 & 0 & b_4 & b_3 \end{pmatrix} \quad (2)$$

giving the determinant,

$$|Q| = (a_1 a_3 - a_2 a_4)(b_1 b_3 - b_2 b_4) = |q_1| |q_2|. \quad (3)$$

The condition $|Q| = 0$ can be satisfied by making either factor, $|q_1|$ or $|q_2|$, equal to zero. This gives four distinct topological phases corresponding to $(\text{Sign} [|q_1|], \text{Sign} [|q_2|]) = (+1, +1), (+1, -1), (-1, +1), (-1, -1)$. Therefore this structure has the classification $2\mathbb{Z}_2$.

It is also apparent from this simple calculation that some of the hopping terms – c_1 and c_2 – do not appear

in the expansion of $|Q|$. This means that the topological classification will be the same as for a structure in which these hopping terms have been set to zero. Physically, removing these links creates two completely separate lattices, the top and bottom loops in Fig.2. We call these the two *sections* of the original structure.

The Hamiltonian, and thus Q , for a separated structure is block diagonal, so the determinant, $|Q|$, is simply a product of the two block determinants, as the expansion shows. The absence of the c terms from the expansion of $|Q|$ is a consequence of the block triangular form of Eq.(2). However, this pattern is only explicit if the sites are ordered correctly, which depends on finding the sections defining the blocks in the matrix. As we prove in the supplementary material section A.1, the determinant is factored if and only if there exists a block triangular form of Q , so finding an appropriate ordering of sites allows us to find the number of sections in a structure.

A graph-theoretic approach to this problem involves enumerating the *complete matchings* of a structure. A complete matching consists of a set of pairings of sites, or *matchings*, which are connected (by a non-zero hopping term), such that every site in the structure is included in exactly one pair. Examples of such complete matchings are shown in Fig. 4, for the four row graphene ribbon which we investigate experimentally in section III. A complete matching has an algebraic interpretation: if we index separately the black and white sites such that each each matched pair has the same index, the corresponding hopping terms appear along the diagonal of the matrix Q . The terms in the expansion of the determinant of a matrix correspond to the product of the diagonal elements for every possible permutation of the columns (or rows). Hence finding the set of complete matchings for a structure gives all the terms in the expansion (to get the signs, it is also necessary to keep track of the number of swaps required to go between matchings). This is the Harary-Sachs theorem [33, 34] for weighted bipartite graphs.

A consequence of the relationship between complete matchings and the expansion of $|Q|$ is that any connection which is not included in any matching does not appear in the expansion, so can be removed to reveal the sections. In the case of the structure in Fig. 4, all the connections between the rows can be removed, so the structure has four sections. For each section, there are two complete matchings, so each factor $|q_i|$ of $|Q|$ contains two terms. Since these have opposite signs, every factor can be made to pass through zero, so the structure has classification $4\mathbb{Z}_2$. Note that even small changes in connectivity can change this completely. If we add just one connection between the a white site of top row and a black site of the bottom row of the structure, we find that there are complete matchings which include every connection, so there are no sections and the classification is \mathbb{Z}_2 .

The relationship between the number of sections of a structure and a block triangular form of Q in Eq.(2) can

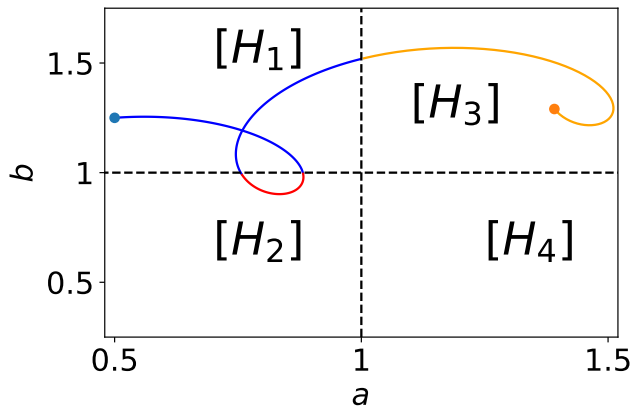


FIG. 3. A slice of the parameter space for 2 row ribbon zigzag graphene, which has the classification $2\mathbb{Z}_2$. This slice is defined by setting all the hopping terms equal to 1, apart from one in each row, a and b , which are allowed to evolve independently. $[H_x]$ denotes a set of topologically equivalent Hamiltonians, and the dashed lines denote phase boundaries. The path shown undergoes 3 phase transitions between the phases $[H_1]$, $[H_2]$, and $[H_3]$, where each phase transition is identified by the appearance of a pair of unavoidable degenerate zero energy states.

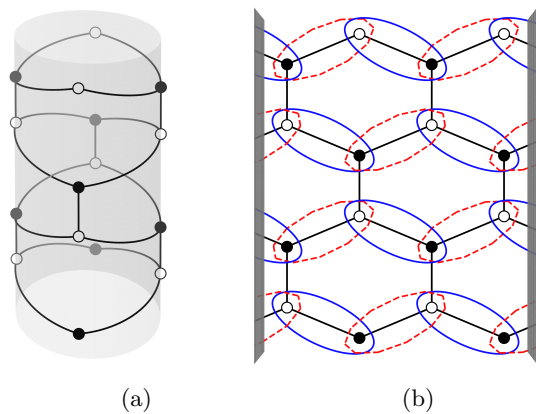


FIG. 4. (a) The four row ribbon graphene structure looped to form a cylinder. (b) The complete matchings of this structure, flattened for clarity. A complete matching consists of a solid or dashed set of matchings from each row. The choice for each row is independent so there are 2^4 complete matchings. The connections between the rows do not appear in any of the matchings, so each row forms a separate section. the topological classification for this structure is $4\mathbb{Z}_2$.

be made rigorous. In the supplementary material section A.1, we prove that the factorisation of $|Q|$ according to sections, $|Q| = \prod_i |q_i|$, can be made if, and only if Q can

be written in the block triangular form

$$Q = \begin{pmatrix} q_j & \cdots & c_{i+1,j} & c_{i,j} \\ & \ddots & \vdots & \vdots \\ 0 & & q_{i+1} & c_{i,i+1} \\ & & & q_i \end{pmatrix}, \quad (4)$$

where the q_i and c_{ij} are matrix blocks. Therefore by finding an appropriate order of the sites the number of sections will be revealed in a structure.

The diagonal blocks, q_i , in Eq.(4) define the sections of the structure. They include the hopping terms which connect the black and white sites within the section. The off diagonal blocks, $c_{i,j}$, contain the connections between the sections. The hopping terms in the off diagonal blocks do not appear in the expansion of $|Q|$. Note that the connecting terms only appear within superdiagonal blocks – the corresponding subdiagonal is necessarily zero. Thus the connections between sections are always between the sublattices. For instance if Q maps from the black to the white sublattice, then only the white sites of g_j may connect to the black sites of g_i . We will make use of this shortly to define a partial ordering of the sections.

The relationship between the block structure of a matrix and the topological classification of a chiral structure has allowed us to find an algorithm to classify a random chiral network. Details of this algorithm are given in the supplementary material section B. Of our classification algorithm, the most numerically expensive part is finding a basis with the largest number of triangular blocks. An alternative algorithm for this part of the classification is detailed in [35] although we have not compared the complexity of our algorithm to this alternative approach.

The factorisation and triangular form of Q tells us more than just the topological classification of the Hamiltonian. Physically the nature of localisation at criticality (that is, at a topological phase boundary) is affected, with nullstates exactly restricted to a particular subset of sections. We consider a structure represented by the graph G , with a section g_i corresponding to the factor q_i . For a topologically marginal chiral structure each nullstate can be localised to the black or white sublattice. If only one section is singular, the black state may be non-zero only on a subset G_b of non-critical sections, and the white state may be non-zero on a subset G_w of non-critical sections. The sets G_w , G_b and the critical section g_c are disjoint, so that the only section with support of both the black and white states is g_c . This non-trivial localisation yields an experimental method to find the classification of a structure, discussed in section III.

To understand this localisation, we define a partial ordering of sections, $(g \in G, \leq)$, which provides the upper triangular form in Eq.(4). We say that $g_i < g_j$, or g_i is lower than g_j , if white sites of g_i connect to black sites of g_j , and $g_i > g_j$, or g_i is higher than g_j , if black sites of g_i connect to white sites of g_j . If the blocks q_i and

q_j can be permuted in Q to swap places on the diagonal in such a way that maintains an upper triangular block matrix Q , then $g_i = g_j$. Otherwise if g_i and g_j are not directly connected, we look to neighbouring sections to define the partial ordering. As the structure is connected, we may always iterate to neighbours of neighbours until we have the partial ordering relationship between any two sections.

In order to demonstrate how the localisation of null-states in a critical section is altered by the partial ordering of sections, consider a 4 section structure where Q has the form

$$Q = \begin{pmatrix} q_1 & c_{12} & c_{13} & 0 \\ 0 & q_2 & 0 & c_{24} \\ 0 & 0 & q_3 & c_{34} \\ 0 & 0 & 0 & q_4 \end{pmatrix} \quad (5)$$

where q_i and $c_{i,j}$ are block matrices. The sections have the partial ordering $g_1 < g_2 = g_3 < g_4$. Suppose that section g_3 is marginal, so $|q_3| = 0$ and $|q_1|, |q_2|, |q_4| \neq 0$. Then there exists a null eigenvector $|\phi\rangle$ such that $q_3 |\phi\rangle = 0$. The solution over all of Q is then given by

$$\begin{pmatrix} q_1 & c_{12} & c_{13} & 0 \\ 0 & q_2 & 0 & c_{24} \\ 0 & 0 & q_3 & c_{34} \\ 0 & 0 & 0 & q_4 \end{pmatrix} \begin{pmatrix} -q_1^{-1} c_{13} |\phi\rangle \\ 0 \\ |\phi\rangle \\ 0 \end{pmatrix} = 0 \quad (6)$$

demonstrating the nullstate can have non-zero support on the black sites of g_1 and g_3 only. Similarly $|q_3^\dagger| = 0$ so we have a similar solution for Q^\dagger where

$$\begin{pmatrix} q_1^\dagger & 0 & 0 & 0 \\ c_{12}^\dagger & q_2^\dagger & 0 & 0 \\ c_{13}^\dagger & 0 & q_3^\dagger & 0 \\ 0 & c_{24}^\dagger & c_{34}^\dagger & q_4^\dagger \end{pmatrix} \begin{pmatrix} 0 \\ 0 \\ |\psi\rangle \\ -(q_4^\dagger)^{-1} c_{34}^\dagger |\psi\rangle \end{pmatrix} = 0 \quad (7)$$

and $q_3^\dagger |\psi\rangle = 0$. Hence this nullstate has non-zero support on the white sites of g_3 and g_4 only. The localisation of the support by sublattices is a direct consequence of the partial ordering, in this example $g_1 < g_2 = g_3 < g_4$. These rules generalise in a straightforward way when there are more sections: the black zero energy state is localised on the marginal section and those lower in the partial ordering, while the white state is confined to the marginal section and those which are higher.

It should be noted that within the critical section itself, for a randomly selected distribution of hopping terms that satisfy the condition for a section to be critical, the zero energy states have, with probability one, support on every site of the section. Proofs of this, and of the general relationship between the factorisation and localisation, are given in the supplementary material section A.1.

It is natural to ask what happens when a structure has more than one critical section. In some instances it is possible to have more than two zero energy states. However, for most structures, for almost all sets of hopping terms,

there remain only two zero energy states when there are multiple critical sections. This is because the null states originating from each critical section must be orthogonal to each other, which imposes additional constraints on the hopping terms, including those which connect the sections. The conditions for such higher nullity will be explored in future work.

III. EXPERIMENTAL DEMONSTRATION OF CLASSIFICATION

To demonstrate the topological classification defined in Section III, we have performed experiments on a coaxial cable network which represents the 4 row ribbon graphene structure of Fig. 4. A network where all coaxial cables have the same transmission time, τ , maps on to a tight binding model [26, 30] where the sites are the junctions in the network. The ‘energy’, ε , is given by $\varepsilon = \cos \omega \tau$ where ω is the driving frequency. This yields a Schrödinger type eigenvalue equation $H\psi = \varepsilon\psi$. Entries in ψ correspond to scaled voltages at the junctions. Up to this scaling factor, individual hopping terms are given by the reciprocal of the impedance of a cable connecting the sites. Swapping between cables of different impedances thus allows us to traverse a structure’s parameter space ξ .

Experimental measurements are made with a vector network analyser (VNA) and takes two forms. From on-site reflectance measurements, we determine the structure’s impedance, the real part of which is proportional to the local density of states (LDOS) at that site [26]. We use this to demonstrate the localisation of the null states. Transmittance measurement give the relationship between the magnitude of a state on two sites. This gives a direct experimental determination of the block triangular form of Q , Eq.(2), and thus the classification of the structure.

1. Measuring the Local Density of States

Measuring the local density of states on every site allows us to characterise the localisation properties of the zero energy states in a marginal structure with multiple sections, of which only one is critical. Fig. 5 displays the LDOS measurements of the disordered looped 4 row ribbon zigzag graphene in Fig. 4. According to the classification of Sec. II, this structure has four non-trivial sections, corresponding to the horizontal rows, so its topological classification is $4\mathbb{Z}_2$. Individual cables are chosen randomly from a binary distribution of 50Ω and 93Ω cables (see more details in supplementary material section C). One section is critical, the second row in the figure, while the other three are not. The localisation of the nullstates is clear: the white state only has significant strength on the top two rows, while the black state appears only on the lower three. This is in agreement

with the predicted localisation, given the ordering of the rows $g_1 > g_2 > g_3 > g_4$.

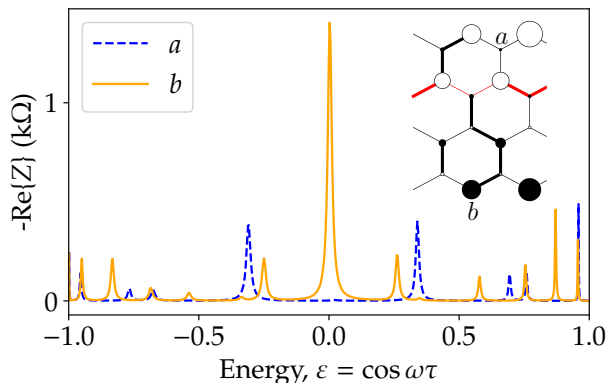


FIG. 5. Experimental measurement of the impedance spectra in a topologically marginal 4 row ribbon graphene structure. The structure has four sections, corresponding to the rows of the structure. Spectra are shown for two sites on the black sublattice, labelled a and b in the structure diagram in the inset. In the plot of the structure the diameter of the circle representing each site is proportional the amplitude of the zero energy state at that point, which is derived from the strength of the corresponding impedance peak. The widths of the lines showing the connections indicates the impedance of the corresponding cable, with wide lines being 93Ω and narrow lines 50Ω cables. The red lines pick out the second row which is the critical section. The localisation of the zero energy eigenstates onto distinct sublattices on the upper and lower sections relative to the critical row agrees with our theoretical prediction. Note that the structure has cylindrical boundary conditions as displayed in Fig. 4 (b), with the hanging connections at either side linked together.

2. Topological Classification through Transmittance

Measurements of the transmittance can be used to verify the triangular form of Q , Eq.(2), and thus the division of the structure into sections. We describe here an experiment where we make a cut in each section of the structure, by disconnecting one end of a cable, and measure transmittance between various cuts. We show that transmittance at zero energy ($\cos \omega\tau = 0$) only occurs when the measurement is within one section: the transmittance between sections is zero.

In order to describe the transmittance of the coaxial cable network, we use a transfer matrix formalism to relate the voltages and currents at the output sites to those at the input sites. If we cut a site on every section (creating an input and output site on each section), the transfer matrix will have dimensions $2\tilde{N} \times 2\tilde{N}$, corresponding to the voltage and current variables for each of the \tilde{N} sections. Here we use \tilde{N} for the total number of sections,

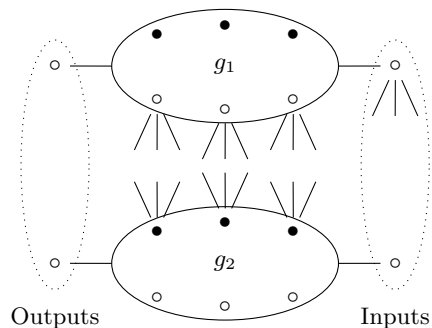


FIG. 6. A structure with two sections, g_1 and g_2 , with the partial ordering of $g_1 < g_2$ since white sites in g_1 connect to black sites in g_2 . The sections correspond to the ellipses, and contain arbitrary numbers of sites, which are not shown individually. The hopping terms connecting the two sections are denoted schematically by bunches of three lines, but they may join any white sites of g_1 to any black sites of g_2 . Each section has been cut to create input and output sites for transmittance measurements.

to distinguish from N , the number of topologically non-trivial sections from earlier.

For a chiral structure at zero energy, all the variables can be coloured black or white, according to the two sublattices, in such a way that the matrix consists of two $\tilde{N} \times \tilde{N}$ diagonal blocks. At zero energy the voltage at a given site is determined entirely by the currents flowing out of the neighbouring sites. The neighbours in a chiral structure are on the other sublattice, so, if we assign the voltage the same colour as its site, and the currents flowing into and out of a site the opposite colour to the site, the variables of the two colours are completely independent, giving the two blocks.

To see how the form of the transfer matrix for the cut structure is related to the sections, consider making a cut within a section, forming an input and output site. The cut adds a site to the structure, unbalancing the black and white sublattices in the section, and thus creating a new zero energy state. For instance cutting on a white site creates one extra white site, resulting in a zero energy state that only has support on the white sites of that section and of any higher sections in the partial ordering. This means that the block triangular form of the matrix Q in Eq.(2) translates to a triangular form of each block of the transfer matrix. This triangular form persists regardless of the site at which the cut is made in each section; it can be shown to exist if, and only if, the uncut structure has at least \tilde{N} sections.

As a simple example, consider a structure with just two sections, g_1 and g_2 , as shown in Fig. 6. The white sites in g_1 connect to the black sites in g_2 , so in the partial ordering, $g_1 < g_2$. Each section is cut at a white site, so the white block of the transfer matrix relates the input and output voltages, while the black block connects the

currents. The transfer matrix is thus

$$\begin{pmatrix} I_{\text{out}}^{g_1} \\ I_{\text{out}}^{g_2} \\ V_{\text{out}}^{g_1} \\ V_{\text{out}}^{g_2} \end{pmatrix} = \begin{pmatrix} \gamma & \delta & 0 & 0 \\ 0 & \beta & 0 & 0 \\ 0 & 0 & \alpha & 0 \\ 0 & 0 & \nu & \mu \end{pmatrix} \begin{pmatrix} I_{\text{in}}^{g_1} \\ I_{\text{in}}^{g_2} \\ V_{\text{in}}^{g_1} \\ V_{\text{in}}^{g_2} \end{pmatrix}, \quad (8)$$

where the non-zero matrix entries represented by Greek letters are functions of the hopping amplitudes in the Hamiltonian, and depend on the details of the actual structure.

It is not possible to measure directly the form of such a transfer matrix using a two-port VNA, which can only give the transmittance between one input and one output site. The voltages and currents at the other input and output sites cannot simply be made zero: we can either leave them open circuit, in which case there can be a voltage on the site, but no current flowing in or out, or they can be shorted, giving a current but no voltage. In our experiment, the output site is always open circuit, and the choice of whether to short or leave open the input site is made according to the partial ordering.

To see how this works, consider the case where the input and output are connected to section g_1 and the input to g_2 is open circuit. Then $I_{\text{in}}^{g_2} = 0$ and $I_{\text{out}}^{g_2} = 0$. From Eq.(8), we get $I_{\text{out}}^{g_1} = \gamma I_{\text{in}}^{g_1}$ and $V_{\text{out}}^{g_1} = \alpha V_{\text{in}}^{g_1}$, so non-zero transmittance occurs. However, if the input to g_2 is shorted, the boundary conditions instead become $V_{\text{in}}^{g_2} = 0$ and $I_{\text{out}}^{g_2} = 0$. This gives $I_{\text{out}}^{g_1} = 0$ and $V_{\text{out}}^{g_1} = \alpha V_{\text{in}}^{g_1}$, so no transmittance can be seen, because this requires both the output voltage and current to be non-zero. Hence, for our classification experiment to work, with intra-section transmittance non-zero, we need the g_2 input site to be open circuit.

Proceeding in the same way, we find that if the input port is connected to the input site of g_1 and the output port to the output site of g_2 , we get non-zero transmittance if the input to g_2 is shorted, but not if it is open circuit. Thus, to see no transmittance between sections, we again need g_2 to be open circuit.

If we do these experiments with input port connected to the input site of g_2 , the requirement is reversed: the g_1 input site has to be shorted to get non-zero transmittance within the section g_2 , and no transmittance between sections g_1 and g_2 . The reason for this difference is the partial ordering of the sections $g_1 < g_2$. However, these rules only work because we have cut the sections on the white sites. Going through the different cases, we find

that the requirement for shorting or leaving open the unused input sites depends on the sublattice of the site and the position of the section in the partial ordering relative to the input site connected to the VNA. These requirements are summarised in Table I. When these rules are satisfied, there is non-zero transmittance between the input and output sites when they are on the same section, but not when they are on different sections. This pattern is a direct consequence of the triangular blocks in the transfer matrix, and does not occur otherwise. For example, in a structure without sections but with two cuts on white sites, shorting one of the input sites results in no transmittance for either output site.

Input site	Higher	Lower	Equal
Black	Short	Open	Open/Short
White	Open	Short	Open/Short

TABLE I. Conditions for shorting or leaving open circuit the inputs to the sections where the input site is not connected to the VNA. The requirements depend on the sublattice which the input belongs to, black or white, and its position in the partial ordering, higher or lower than the connected section. With these choices, non-zero transmittance occurs only when the output site is in the same section as the input.

Having established these rules, we use transmittance measurements to verify the presence of the sections in the looped four row zigzag graphene ribbon shown in Fig. 4 (which has been used as an example elsewhere in this paper). Recall that this structure has four sections, corresponding to the four rows of sites. Where the subscript of each row is sequentially labelled, the partial ordering of the sections is $g_1 > g_2 > g_3 > g_4$. A cut is made in each row, so the looped structure is transformed into a sheet, shown in Fig. 7 (a), creating an extra site on each row. Note, however, that the sections we find correspond to the uncut loop rather than the sheet. In two of the sections, the cut is on a white site, while in the other two the site is black. We perform transmittance measurements going through the four output sites, and measuring a spectrum for every input sites in each case. The rules in Table I determine whether the unconnected input sites are left open circuit or shorted. For example, when the VNA is connected to the input site on the second row, the first row, which is higher in the ordering and has a white input site, is left open, while the third and fourth rows are, respectively, shorted and open circuit. Using the transfer matrix for the clean structure, where all the cables have impedance $Z_0 = 50\Omega$, this input gives

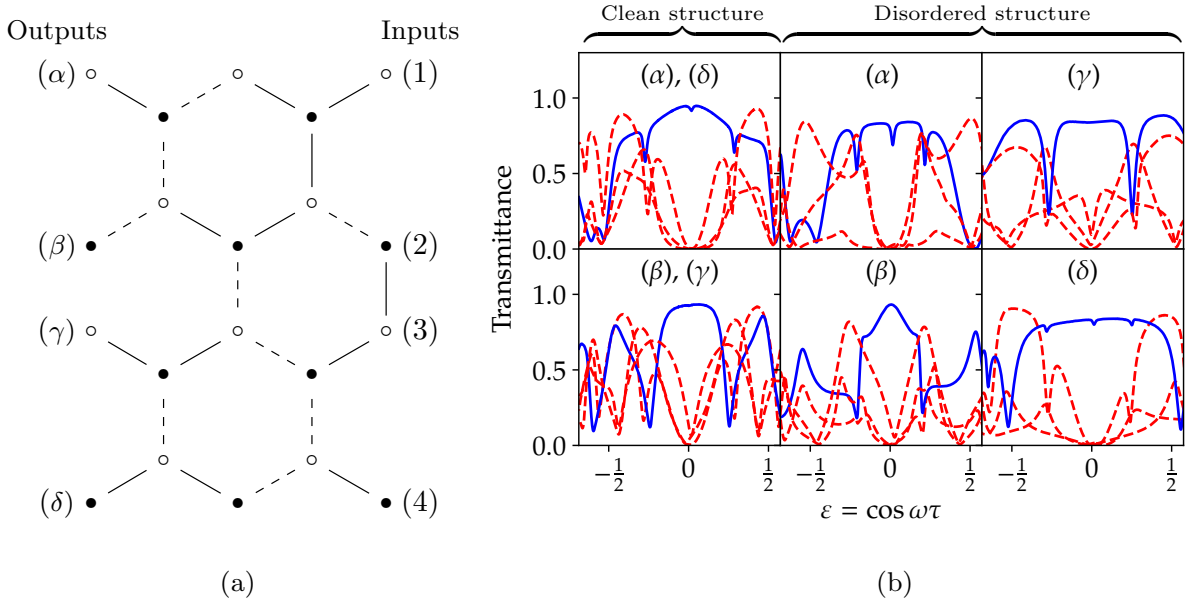


FIG. 7. (a) The looped four row zigzag ribbon structure cut so it forms a flat sheet. The looped structure is predicted to consist of four sections, corresponding to the four rows of sites. Input sites for the transmittance measurements are labelled on the right hand side, and outputs on the left hand side. For the disordered structure, dashed lines indicate 93 Ω RG62 cables, while solid lines indicate 50 Ω RG58 cables. The clean structure had only 50 Ω RG58 cables. (b) Experimental transmittance data. Each subplot corresponds to a different output site according to the labels in (a), with spectra shown for all four inputs in each case. The blue spectrum is for the case where the input and output site are on the same section, with the dashed red spectra corresponding to transmittance between sections. The transmittance at zero energy is expected to be zero if the input and output sites are in different sections, but non-zero when they are in the same section. The experiment thus confirms that each row is a separate section.

$$\begin{pmatrix} V_{\text{out}}^{g_1} \\ I_{\text{out}}^{g_2} \\ V_{\text{out}}^{g_3} \\ I_{\text{out}}^{g_4} \\ I_{\text{out}}^{g_1} \\ V_{\text{out}}^{g_2} \\ I_{\text{out}}^{g_3} \\ V_{\text{out}}^{g_4} \end{pmatrix} = \begin{pmatrix} 1 & Z_0 i & -1 & -Z_0 i \\ 0 & 1 & \frac{1}{Z_0} i & -1 \\ 0 & 0 & 1 & Z_0 i \\ 0 & 0 & 0 & 1 \\ & & & & 1 & 0 & 0 & 0 \\ & & & & Z_0 i & 1 & 0 & 0 \\ & & & & -1 & \frac{1}{Z_0} i & 1 & 0 \\ & & & & -Z_0 i & -1 & Z_0 i & 1 \end{pmatrix} \begin{pmatrix} V_{\text{in}}^{g_1} \\ I_{\text{in}}^{g_2} \\ 0 \\ 0 \\ 0 \\ V_{\text{in}}^{g_2} \\ I_{\text{in}}^{g_3} \\ V_{\text{in}}^{g_4} \end{pmatrix} = \begin{pmatrix} V_{\text{in}}^{g_1} + Z_0 i I_{\text{in}}^{g_2} \\ I_{\text{in}}^{g_2} \\ 0 \\ 0 \\ 0 \\ V_{\text{in}}^{g_2} \\ I_{\text{in}}^{g_3} + \frac{1}{Z_0} i V_{\text{in}}^{g_2} \\ V_{\text{in}}^{g_4} + Z_0 i I_{\text{in}}^{g_3} - V_{\text{in}}^{g_2} \end{pmatrix}. \quad (9)$$

For the disordered structure, the blocks of the matrix are still triangular, but the expression for the elements are more complicated. The numerical value for this matrix is given in the supplementary material section C.

If the other port of the VNA is not attached to the output site on the second row, it is left open circuit, that is $I_{\text{out}}^{g_2} = 0$. However, this forces $I_{\text{in}}^{g_2}$ also to be zero, so no current enters the structure, and no transmittance occurs. However, for the output on the same row, $I_{\text{out}}^{g_2} = I_{\text{in}}^{g_2}$ and $V_{\text{out}}^{g_2} = V_{\text{in}}^{g_2}$, so, in the absence of absorption, there is a perfect transmittance of 1.

The transmittance experiment was carried out twice, first using a ‘clean’ structure with all 50 Ω (RG58) cables, and then for a disordered structure where hopping terms were randomly selected from a binary distribution of 50 Ω (RG58) and 93 Ω (RG62) cables, identical to the one in

Sec. III 1. The clean structure has reflection symmetry about a line between the second and third rows, so we need only need to use two outputs, α and β (labelled in Fig.7 (a)), but in each case we measure transmittance for all four input sites. In the disordered structure this symmetry is broken, requiring measurements for every input and output site in order to complete the experiment.

The measured transmittance spectra are shown in Fig. 7 (b). Each panel shows data for a particular output site, with the four spectra corresponding to the different input sites. As predicted, in both the clean and disordered structures, the transmittance at $\varepsilon = \cos \omega \tau = 0$ is non-zero only when the output site is on the same section as the input (blue curves). This confirms that the structure has 4 sections, experimentally verifying the $4\mathbb{Z}_2$ classification of this structure. The actual value of the

zero-energy transmittance between the sites within the section is determined by how close the section is to being topologically marginal. For a marginal section, the ideal transmittance, in the absence of losses, would be expected to have a value of unity [26]. Although the differences are not great, it can be seen that the transmittance is highest in the clean structure, where all the sections are marginal, and for the second row section of the disordered structure (output (b)), which is also marginal.

As the structure has chiral symmetry, we expect a symmetry in the transmittance spectra around zero energy. The slight asymmetry in the data is mainly a result of losses in the cables, which have more effect at higher frequencies, but there is also some chiral symmetry breaking due to imperfections in the structure. These necessarily occur because the mapping of the coaxial cable structure to the tight binding model requires the sections of cable between the sites to be of uniform impedance. However, the SMA connectors which form the junctions between the cables are 50Ω components, so for the connections with 93Ω cables this uniformity is necessarily unachievable. As a result, the symmetry breaking is generally greater for the disordered structure than the clean one, where minor variations in the cable lengths are the likely cause.

IV. CONCLUSION

We have described an approach to determining exact topological phases in finite chiral structures, identifying the phase boundaries by the appearance of degenerate pairs of zero energy states. This has been shown, in many cases, to lead to a rich topological classification, obtained by finding a division into sections which correspond to irreducible factors of the determinant of the Hamiltonian. The topological classification is then $N\mathbb{Z}_2$, where N is the number of topologically non-trivial sections or factors. The sections can be identified using the complete matchings of the underlying structure, relating the topological classification to the structures underlying connectivity. Each complete matching is related to a term in the expansion of the determinant, so a hopping term which does not appear in any matching can

be omitted without changing the determinant. The sections correspond to parts of the structure which become separated when these connections are removed. We also give, in section B of the supplementary material, a simple computational algorithm for finding the sections of a structure.

We have defined a partial ordering of the sections in a structure which gives rise to an unusual localisation of the zero energy states which are present when one of the sections is topologically marginal. The zero energy states can be separated so they each have support on a single sublattice. With our definition, the white state is confined to the marginal section and those which are higher in the ordering, while the black state appears on the marginal section and lower sections. This localisation can be seen as a property of finite structures which has some equivalence to the bulk boundary correspondence in infinite structures.

This localisation provides a way in which the sections, and corresponding topological classification can be demonstrated experimentally. We have performed such experiments on simple coaxial cable networks which map directly onto chiral tight binding models. When we make one section marginal, we can use impedance measurements to map out the local density of states on each site. This provides a direct demonstration of the predicted localisation related to the partial ordering. Even without a marginal section, we can use transmittance measurements to show that the structure separates into the expected sections. We have used this method to confirm the $4\mathbb{Z}_2$ classification which our theory predicts for a four row ribbon graphene structure.

ACKNOWLEDGEMENTS

We are enormously grateful for help in the experimental work from Qingqing Duan, Ben Kinvig, and Elena Callus, and also to Belle Darling and Phillip Graham for huge help in finding space to run the experiments. Many thanks also to Patrick Fowler, Barry Pickup, Qingqing Duan, Ben Kinvig, and Elena Callus for many illuminating and insightful discussions while completing this work.

-
- [1] B.-H. Chen and D.-W. Chiou, An elementary rigorous proof of bulk-boundary correspondence in the generalized Su-Schrieffer-Heeger model, *Physics Letters A* **384**, 126168 (2020).
 - [2] D. J. Thouless, M. Kohmoto, M. P. Nightingale, and M. den Nijs, Quantized Hall Conductance in a Two-Dimensional Periodic Potential, *Phys. Rev. Lett.* **49**, 405 (1982).
 - [3] F. D. M. Haldane, Model for a Quantum Hall Effect without Landau Levels: Condensed-Matter Realization of the ‘‘Parity Anomaly’’, *Phys. Rev. Lett.* **61**, 2015 (1988).
 - [4] M. Büttiker, Absence of backscattering in the quantum Hall effect in multiprobe conductors, *Phys. Rev. B* **38**, 9375 (1988).
 - [5] Z. Wang, Y. Chong, Y. Chong, J. D. Joannopoulos, and M. Soljačić, Observation of unidirectional backscattering-immune topological electromagnetic states, *Nature* **461**, 772 (2009).
 - [6] E. Prodan, *Bulk and Boundary Invariants for Complex Topological Insulators: From K-Theory to Physics* (Springer International Publishing, 2016).

- [7] B. Simon, Holonomy, the Quantum Adiabatic Theorem, and Berry's Phase, *Phys. Rev. Lett.* **51**, 2167 (1983).
- [8] A. Kitaev, Periodic table for topological insulators and superconductors, *AIP Conference Proceedings* **1134**, 22 (2009), https://pubs.aip.org/aip/acp/article-pdf/1134/1/22/11584243/22_1_online.pdf.
- [9] A. Altland and M. R. Zirnbauer, Nonstandard symmetry classes in mesoscopic normal-superconducting hybrid structures, *Phys. Rev. B* **55**, 1142 (1997).
- [10] J. Cano, B. Bradlyn, Z. Wang, L. Elcoro, M. G. Vergniory, C. Felser, M. I. Aroyo, and B. A. Bernevig, Building blocks of topological quantum chemistry: Elementary band representations, *Phys. Rev. B* **97**, 035139 (2018).
- [11] B. Bradlyn, L. Elcoro, J. Cano, M. G. Vergniory, Z. Wang, C. Felser, M. I. Aroyo, and B. A. Bernevig, Topological quantum chemistry, *Nature* **547**, 298 (2017).
- [12] C. Brouder, G. Panati, M. Calandra, C. Mourougane, and N. Marzari, Exponential Localization of Wannier Functions in Insulators, *Phys. Rev. Lett.* **98**, 046402 (2007).
- [13] M. G. Vergniory, L. Elcoro, C. Felser, N. Regnault, B. A. Bernevig, and Z. Wang, A complete catalogue of high-quality topological materials, *Nature* **566**, 480 (2019).
- [14] E. Prodan, Disordered topological insulators: a non-commutative geometry perspective, *Journal of Physics A: Mathematical and Theoretical* **44**, 113001 (2011).
- [15] E. Prodan, Non-commutative Brillouin Torus, in *A Computational Non-commutative Geometry Program for Disordered Topological Insulators* (Springer International Publishing, Cham, 2017) pp. 25–48.
- [16] I. Mondragon-Shem, T. L. Hughes, J. Song, and E. Prodan, Topological Criticality in the Chiral-Symmetric AIII Class at Strong Disorder, *Phys. Rev. Lett.* **113**, 046802 (2014).
- [17] T. A. Loring, K-theory and pseudospectra for topological insulators, *Annals of Physics* **356**, 383 (2015).
- [18] A. Cerjan and T. A. Loring, Local invariants identify topology in metals and gapless systems, *Phys. Rev. B* **106**, 064109 (2022).
- [19] R. Bianco and R. Resta, Mapping topological order in coordinate space, *Phys. Rev. B* **84**, 241106 (2011).
- [20] U. Gebert, B. Irsigler, and W. Hofstetter, Local Chern marker of smoothly confined Hofstadter fermions, *Phys. Rev. A* **101**, 063606 (2020).
- [21] A. M. Cook and A. E. B. Nielsen, Finite-size topology, *Phys. Rev. B* **108**, 045144 (2023).
- [22] R. Flores-Calderon, R. Moessner, and A. M. Cook, Time-reversal invariant finite-size topology, *Phys. Rev. B* **108**, 125410 (2023).
- [23] N. Marzari, A. A. Mostofi, J. R. Yates, I. Souza, and D. Vanderbilt, Maximally localized Wannier functions: Theory and applications, *Rev. Mod. Phys.* **84**, 1419 (2012).
- [24] N. Marzari and D. Vanderbilt, Maximally localized generalized Wannier functions for composite energy bands, *Phys. Rev. B* **56**, 12847 (1997).
- [25] H. Zhang and A. Kamenev, Anatomy of topological anderson transitions, *Phys. Rev. B* **108**, 224201 (2023).
- [26] D. M. Whittaker, M. M. McCarthy, and Q. Duan, Observation of a Topological Phase Transition in Random Coaxial Cable Structures with Chiral Symmetry (2023), arXiv:2311.11040 [cond-mat.dis-nn].
- [27] S.-J. Choi and B. Trauzettel, Stacking-induced symmetry-protected topological phase transitions, *Phys. Rev. B* **107**, 245409 (2023).
- [28] A. García-Fuente, D. Carrascal, G. Ross, and J. Ferrer, Full analytical solution of finite-length armchair/zigzag nanoribbons, *Phys. Rev. B* **107**, 115403 (2023).
- [29] R. K. Malakar and A. K. Ghosh, Engineering topological phases of any winding and Chern numbers in extended Su-Schrieffer-Heeger models, *J. Phys.: Condens. Matter* **35**, 335401 (2023).
- [30] D. M. Whittaker and R. Ellis, Topological Protection in Disordered Photonic Multilayers and Transmission Lines (2021), arXiv:2102.03641 [physics.optics].
- [31] T. Jiang, M. Xiao, W. Chen, L. Yang, Y. Fang, W. Y. Tam, and C. T. Chan, Experimental demonstration of angular momentum-dependent topological transport using a transmission line network, *Nat Commun* **10**, 10.1038/s41467-018-08281-9 (2019).
- [32] C. Oliver, D. Nabari, H. M. Price, L. Ricci, and I. Carusotto, Photonic lattices of coaxial cables: flat bands and artificial magnetic fields (2023), arXiv:2310.18325 [physics.optics].
- [33] F. Harary, The Determinant of the Adjacency Matrix of a Graph, *SIAM Review* **4**, 202 (1962).
- [34] H. Sachs, Beziehungen zwischen den in einem Graphen enthaltenen Kreisen und seinem charakteristischen Polynom., *Publ. Math. Debrecen* **11**, 119 (1964).
- [35] I. S. Duff and B. Uçar, On the Block Triangular Form of Symmetric Matrices, *SIAM Review* **52**, no. 3, 455–470 (2010).
-

Supplementary Materials: A Topological Classification of Finite Chiral Structures using Complete Matchings

A. FACTORISATION THEOREM

In this section we prove a theorem relating the triangular block form of Q to the factorisation of $|Q|$. Consider a real or complex matrix Q , where Q is a chiral block of a Hamiltonian

$$H = \begin{pmatrix} 0 & Q \\ Q^\dagger & 0 \end{pmatrix}. \quad (\text{S1})$$

Below we show that, for algebraically independent hopping terms, then $|Q|$ is reducible if and only if there exists a way of ordering the sites such that Q is upper block triangular. We refer to the resultant form of Q as the maximal triangular block basis, or triangular block basis of Q , but it should be emphasised that this basis specifically corresponds to a permutation of H . We will use this in section B to define an algorithm that classifies a particular structure.

Note that often in the following arguments we will refer to a property that occurs *almost always*. By this we mean that if hopping terms were selected randomly from a continuous distribution (possibly one that satisfies a certain constraint) then this property occurs with probability 1.

We proceed by showing that the factorisation is well defined, before proving that a square weighted matrix has a factored determinant (for all matrix entries) if and only if it is block triangular. In proving this relationship we will show that when a section is singular, for almost all hopping terms a section has non-zero support of an eigenstate on all sites.

In order to interpret determinants of a matrix as a polynomial, we consider a polynomial ring that contains them. Formally this ring is larger than the set of polynomials corresponding to determinants, but this is unimportant for our discussion. In particular we are interested in determinants of matrices, so we consider an $N \times N$ matrix,

$$Q_{i,j} = X_{i,j} \quad (\text{S2})$$

where $X_{i,j}$ is an indeterminate over some field, or else fixed at 0, and all non-zero $X_{i,j}$ are algebraically independent. Generically we take this to be \mathbb{R} or \mathbb{C} , but more arbitrary fields are perfectly reasonable to consider. We then take the polynomial ring $P[X_{i,j}]$ over the indeterminates $X_{i,j}$. The determinants $|Q|$ are polynomials in this ring which are linear for each hopping term in $|Q|$. To consider the matrices that may only represent tight binding models undergoing continuous evolution, then we need to restrict the domain for each indeterminate to be \mathbb{R}^\pm or $\mathbb{C} \setminus \{0\}$ or else fixed at 0. Non-zero indeterminates are then in a semiring.

Formally when we classify a structure we are interested in the subspace E_0 of ξ which has no (exactly) zero energy states. We then wish to calculate the number of ways we can map a Hamiltonian to this subspace, which corresponds to calculating the zeroth homotopy group of E_0 under the usual topology. The zeroth homotopy group of a space counts the number of disconnected components of that space. The irreducible factorisation of $|Q|$ tells us the number of path connected components in E_0 .

Definition A.1. Let X be the subspace of ξ corresponding to a solution to $|Q| = 0$. Then $E_0 := \xi \setminus X$.

In order for our classification to be well defined, we need there to exist a factorisation of $|Q|$ that is irreducible and unique, that is we need the polynomial ring to be prime. This follows directly from the fact that the indeterminates are taken over a field. In other words P is a unique factorisation domain. For a less abstract argument, consider the following:

Proposition A.2. If for some hopping terms $|Q| \neq 0$ then $|Q|$ has a unique irreducible factorisation in P .

Proof. Suppose $|Q| = \prod a_i$ and $|Q| = \prod b_i$ such that a_i, b_i are irreducible. Assume that for the irreducible factor a_j there is no irreducible factor b_k such that $a_j = mb_k$ for some non zero constant m , then

$$\prod_{i \neq j} a_i \neq \frac{\prod_{i \neq k} b_i}{m}. \quad (\text{S3})$$

multiplying by $a_j = mb_k$ we see

$$a_j \prod_{i \neq j} a_i \neq b_k \prod_{i \neq k} b_i \quad (\text{S4})$$

which is a contradiction. Hence for every j there is a k such that $a_j = mb_k$ for some constant m , showing a factorisation of $|Q|$ is unique and irreducible. \square

Given that the irreducible factorisation of $|Q|$ is well defined, we now give a proof that $|Q| = \prod |q_i|$ if and only if there exists a block triangular structure of Q with q_i as diagonal blocks.

A.1.

Here we aim to prove that a determinant of Q is factored if and only if there exists a block triangular basis of Q . A corollary of one of the propositions is that a critical section almost always has non-zero support of the nullstates on every site. To prove this we first show that two sections, pairwise, may only connect on one sublattice. Then we show that for a structure with N sections there must always be at least one section that may only connect to any other section on one sublattice. As this is true for any number of sections N this implies that if $|Q|$ is factored, then there exists a triangular block structure of Q .

More specifically, given a section g_i , if every first minor of q_i is almost always non-zero then deleting a black and a white site from g_i will result in a structure with a complete matching, because the determinant of the remaining structure is almost always non-zero. Therefore if we have two sections, g_i and g_j and they connect to one another on both sub lattices, then we can delete a black and a white site from both sections (each) that are connected to one another. The remaining structure has a complete matching because the associated minor is factored by a first minor of q_i and a first minor of q_j . Consequently g_i and g_j can connect to one another on only one sublattice.

Our proof relies on knowing when hopping terms are in a complete matching of some graph or not. For this we need to define a type of matching.

Definition A.3. A **valid matching** is a matching between two sites on some graph g such that the matching is part of a complete matching of g .

We then show that there cannot exist a particular type of cycle of sections (see Definition A.8). This ensures at least one section can only connect to other sections from one sublattice. This is true for an arbitrary number of sections, giving the triangular structure to Q .

For consistency if two sections g_i and g_j connect from a black site in g_i to a white site in g_j we say g_i connects to g_j on the black sub lattice.

Proposition A.4. Given a section g_i with tight binding model $h_i = \begin{bmatrix} 0 & q_i \\ q_i^\dagger & 0 \end{bmatrix}$ such that $|q_i|$ is irreducible, then every first minor of q_i is almost always nonzero.

Proof. Given that h_i is chiral, a non-zero term in $|q_i|$ corresponds to a complete matching of g_i . Any first order minor of q_i can be accessed by deleting a white and a black site from g_i , with the first order minors corresponding to determinants of the $(N-1) \times (N-1)$ sub matrices of q_i . So if there exists a complete matching of every structure where we delete a black and a white site from g_i then for almost all hopping terms the minor is non-zero.

Suppose that we have a section with the set of complete matchings $\mathcal{C} = \{C_i\}$ and delete a black site b_1 . Match all the remaining sites possible from the complete matching C_i , leaving a single unmatched white site w_1 . If an individual site is in only one valid matching, as every complete matching must include a matching on every site, this would factorise the determinant. So every site is in at least two distinct valid matchings contained in the complete matchings \mathcal{C} . So w_1 may be matched to a black site b_2 with a matching in C_j . Removing the matching containing b_2 which is in the complete matching C_i leaves a second white site w_2 unmatched. This process has changed which site is the unmatched white site, see Fig. S1 for an example. Iterating this step defines a walk over the structure. If we delete the unmatched white site, we automatically get a complete matching of the remaining structure, showing the associated minor is almost always non-zero.

We now demonstrate any white site in a section may be unmatched by such a walk. Assume there are a set \mathcal{W}_m of white sites that cannot be unmatched by iterating this walk, and a set \mathcal{W}_u of white sites that can be unmatched by iterating this walk. In C_i all \mathcal{W}_m white sites are matched to a black site. If there exists a valid matching from a black site b_1 to a white site in \mathcal{W}_m and a valid matching from b_1 to a white site in \mathcal{W}_u , then the site in \mathcal{W}_m is unmatchable. So the black neighbours of \mathcal{W}_m sites do not have a valid matching to any white site in \mathcal{W}_u . If a white site has a valid matching to b_1 it is possible to unmatch, so no white site $w_m \in \mathcal{W}_m$ has a valid matching to b_1 . This partitions the sites in to two sets: one with white sites that can be unmatched U , and one with white sites that cannot be unmatched M , with valid matchings. The valid matchings over M are therefore independent of the valid matchings over U , giving a factorisation of $|q_i|$. By contradiction all white sites in a section are possible to unmatch via such a walk. As the choice of b_1 was arbitrary, this proves the existence of a complete matching of a section when deleting one white and one black site, that is, every first minor of $|q_i|$ is non-zero. \square

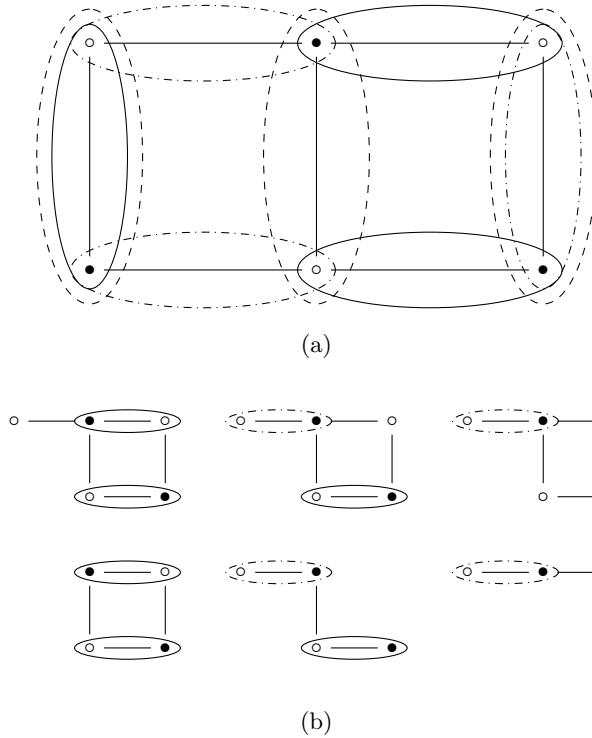


FIG. S1. (a) 3 rung ladder graphene, which has the classification \mathbb{Z}_2 , and all 3 complete matchings of the structure denoted with a solid line, dashed line, and dash dot line. (b) Displays the structure having deleted one of the black vertices, and matching all but one white vertex. By swapping a single matching that neighbours the unmatched vertex at a time, it is possible to leave any of the white sites unmatched. Deleting the unmatched white vertex shows that for the deleted black vertex, deleting any of the white vertices leaves a structure with a complete matching.

Corollary A.5. Suppose a section is singular, then $q_i |\psi\rangle = 0$ for some non-zero $|\psi\rangle$, and for almost all hopping terms $|\psi_j\rangle$ indexed over the j sites of g_i is non-zero for every j .

Proof. By Prop. A.4 every first minor of q_i is almost always non-zero. Therefore any submatrix \bar{q}_i resulting from deleting a white and black site of g_i is almost always non-singular. Projecting the eigenstate $q_i |\psi\rangle = 0$ on to the submatrix gives

$$\bar{q}_i |\bar{\psi}\rangle \neq 0 \quad (\text{S5})$$

for all \bar{q}_i . Therefore given any submatrix of $[\bar{q}_i \ \alpha]$ of q_i such that

$$q_i = \begin{bmatrix} \bar{q}_i & \alpha \\ & A \end{bmatrix} \quad (\text{S6})$$

and $|\psi\rangle = \begin{bmatrix} |\bar{\psi}\rangle \\ |\psi_\alpha\rangle \end{bmatrix}$ for $q_i |\psi\rangle = 0$

we see

$$\bar{q}_i |\bar{\psi}\rangle = -\alpha |\psi_\alpha\rangle. \quad (\text{S7})$$

As every first minor is non-zero then for almost all hopping term values $|\psi\rangle$ has non-zero support on every site of g_i . \square

We now wish to show that, given a pair of sections g_i, g_j then they may only connect on one sublattice.

Proposition A.6. Given two section g_i, g_j then non-zero hopping terms may only be between black sites on g_i to white sites on g_j .

Proof. Given two sections g_i, g_j assume they connect to one another on both sublattices. Delete four sites, a black and a white site in g_i and a white and a black site in g_j that connect to the original white and black site g_i . By Prop. A.4 the resulting structure has a complete matching. Therefore if we put back in the four deleted sites, and match them via their associated hopping terms, then there exists a complete matching of g_i and g_j that is not factored by $|q_i|$ and $|q_j|$. So by contradiction g_i and g_j connect on only one sublattice. \square

To show that given N sections there exists a section which can only connect to any other section from one sub lattice, we first define an edge section.

Definition A.7. An **edge section** is a section that may only connect to all other sections from one sub lattice.

To prove there always exists an edge section we consider a cycle of sections.

Definition A.8. A **section cycle** is a path through a subset of sections in G such that it starts and ends on the same section following hopping terms in g_i and leaves each section on a different sub lattice to the one it entered on.

We now show there cannot exist a section cycle.

Proposition A.9. A section cycle cannot exist in any structure.

Proof. Suppose every section is in a cycle, then every section connects to a distinct section on both sub lattices. For each distinct section cycle we can delete a pair of sites, one black and one white, from each section in the cycle such that the black and white sites connect to different sections in the cycle. By Prop. A.4 the resulting structure has a complete matching. Putting back in the deleted sites and hopping terms, we can now construct a complete matching that is not factored by any of the sections in that cycle. Therefore by contradiction there exist no section cycles. \square

Corollary A.10. In a structure with N sections there exists at least one edge section.

Proof. Suppose every section g_i connects to at least one other section g_j on the white sub lattice and one different section g_k on the black sub lattice. Given such a requirement, then if no edge section exists there must be at least $N + 1$ sections. Therefore by the pigeonhole principle, if every section connects on both sub lattices a section cycle exists, which is not possible by Prop. A.8 giving a contradiction. \square

We now wish to show that the existence of an edge section gives the triangular basis to Q .

Theorem A.11. If $|Q| = \prod |q_i|$ for $|Q|, |q_i| \in P[X_{i,j}]$ then there exists a permutation of H that gives a triangular block basis for Q .

Proof. Given a structure with N sections then by corollary A.10 there is at least one section, g_1 , which only connects to all others from one sub lattice. Taking G and deleting g_1 yields a new structure, \bar{G} , with $N - 1$ sections. By corollary A.10 this structure also has an edge section g_2 . This may be iterated until only one section remains. This gives the partial ordering of the structure and therefore defines a triangular block basis of Q . \square

B. A CLASSIFICATION ALGORITHM

We present an algorithm to find the classification of a structure based on Theorem A.11. That is, we take some input structure, with a chiral Hamiltonian and find an ordering of the sites where Q is block triangular, and every diagonal block corresponds to a section of the structure. We refer to the corresponding basis as the **maximal triangular block basis** of Q . Then, given the domain of each hopping term and numerical bounds on the determinant, we check if a section is trivial or not. We anticipate that this algorithm can be significantly optimised, but currently we are able to analyse up to random networks with around 50 sites. Of course, given a more consistent underlying lattice structure it often makes sense to classify a large (say many thousand sites or more) system by proving some simple results about the complete matchings of that lattice, coupled with some boundary conditions.

There are two main parts of the algorithm: to find a triangular block basis of Q with all sections on the diagonal, and then to classify each section. The former is more technically challenging. The first part uses the fact that to get a triangular block structure to an $N \times N$ size Q there needs to be a $j \times (N - j)$ block of zeros, so by taking the complement of Q (with all unit hopping terms) then we can find overlaps in zeros by taking dot products between column vectors, or a generalised product over several column vectors. The generalised product is defined as follows.

Definition B.1. The generalised product of N column vectors $\{c^i\}$ is given by

$$p = \sum_j \prod_i c_j^i \quad (\text{S8})$$

where j denotes the j th entry of the column vector c^i .

Given $N - j$ columns, if $p \geq j$ then there is a $j \times (N - j)$ block of zeros in Q . The algorithm then follows the following general outline

1. Compute Q° where $Q_{i,j}^\circ = 1$ if $Q_{i,j} = 0$, otherwise $Q_{i,j}^\circ = 0$
2. Check for $1 \times (N - 1)$ blocks of zeros by checking $\sum_i Q_{i,j}^\circ$ for every j . Take indices of all blocks of this size.
3. Find pairwise overlap matrix, A , of two column vectors of $Q_{i,j}^\circ = 1$,

$$A_{i,j} = \sum_k Q_{k,i}^\circ Q_{k,j}^\circ \quad (\text{S9})$$

4. If any $A_{i,j} \geq N - 2$ there is a $2 \times (N - 2)$ block of zeros. Take indices of all blocks of this size.
5. For $j \geq 2$ take all columns that have overlap greater than $N - j$. If number of columns with such an overlap $\geq N - j$ set Check = 1.

If Check==1:

For all combinations of $N - j$ columns with pairwise overlap $\geq N - j$ compute p .

If $p \geq N - j$ return indices of $j \times (N - j)$ block of zeros.

A simple way to optimise this algorithm slightly is to project on to a sub matrix of Q that excludes any individual section, whenever a relevant $j \times (N - j)$ block of zeros is found. Then the combinations of column vectors that need to be checked to find more blocks of zeros is significantly smaller. Furthermore the complexity of the search scales with the number of potential column vectors to check. So if the search for zero blocks can be done up until $j \leq \frac{N}{2}$ for the column vectors, and then switched to do a search over the remaining row vectors the algorithm may be faster.

The second part of the algorithm is much simpler, and only applies when hopping terms are restricted to being real. By the fundamental theorem of algebra if all hopping terms are complex then a solution to $|q_i| = 0$ always exists for at least a 2×2 size block q_i corresponding to a section. For hopping terms restricted to \mathbb{R}^\pm we require some more computation. The first part of the algorithm computes the number of sections of Q , and by indexing blocks of zeros finds a maximal triangular block basis for Q . So we now need to see if each factor can be set to 0. This works by considering bounds for the largest value of $|q_i|$ for all $|u| \in (0.5, 1]$ hopping terms, where the sign of u set by the domain of that individual hopping term (i.e. if $u \in \mathbb{R}^+$ then $u > 0.5$ and if $u \in \mathbb{R}^-$ then $u < -0.5$). All hopping terms are then selected as a random float in $\pm(0.5, 1]$, and it is checked if this gives a singular section, if not we proceed, otherwise we reselect randomly reselect hopping terms. Suppose all hopping terms in q_i are non-zero, then by Prop. A.4 every hopping term appears in the expansion of $|q_i|$. The maximum number of non-zero terms in the determinant of an $N \times N$ matrix is $N!$ and so $|q_i| \leq N!$. Therefore if a particular hopping term, a , is left free to vary then $|q_i| = aA + B$. If solutions to $|q_i| = 0$ exist for some a then for $|a| \times (0.5)^{N-1} > (N - 1)!$ and $|q_i|$ has one sign, and for $a = 0$ then $|q_i| = B$ and has a different sign. This is then repeated for every hopping term until a solution is shown to exist, or it is shown to not exist for all sections. That is

1. Randomly select all hopping terms u so that $|u| \in (0.5, 1]$ and the sign corresponds to the domain of that hopping term. If $|q_i| \neq 0$ proceed, otherwise randomly reselect all hopping terms until $|q_i| \neq 0$.
2. Keeping the hopping terms as in the first step set $a = \pm 2^N (N - 1)!$ where the sign is specific to the domain of a . Calculate $\text{Sign}(|q_i|)$.
3. Keeping the hopping terms as in the first step set $a = 0$ where the sign is specific to the domain of a . Calculate $\text{Sign}(|q_i|)$.
4. If a change of sign is found:

Return section non-trivial

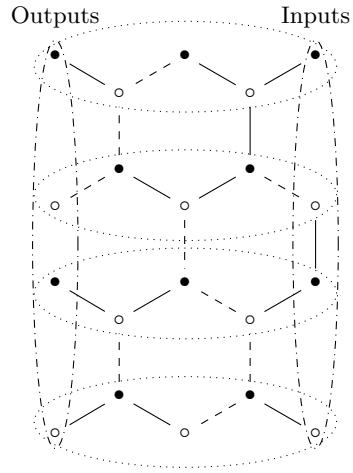


FIG. S2. The disordered structure the transmittance experiment was performed on, as discussed in section III 2 of the paper, with sites in each section already cut for measurements. The dashed lines denote the 93Ω RG62 cables, and the solid lines denote 50Ω RG58 cables. The same structure with all 50Ω RG58 cables is the clean structure used for the transmittance experiments. The dash-dotted ellipses denote the input and output sites. The same structure with uncut sites was used for the localisation experiment in section III 1 of the paper. This structure has 4 sections and a $4\mathbb{Z}_2$ classification.